Indian Journal of Chemical Technology
Vol. 26, January 2019, pp. 23-34

Dye adsorption efficiency of chemically treated activated carbon based on sugarcane bagasse pith

Manisha Ahire & Sunil Bhagwat*

Department of Chemical Engineering, Institute of Chemical Technology, Matunga (E), Mumbai 400 019, India.

E-mail: ss.bhagwat@ictmumbai.edu.in

Received 3 March 2016; accepted 5 August 2018

The adsorption capacity of a cationic dye (Methylene blue, MB) from aqueous solution onto activated carbon prepared from sugarcane bagasse pith (*Saccharum Officinarum*) has been investigated. Activated carbon is prepared from sugarcane bagasse pith (SBP) using chemical activation method. This method involves impregnation with ferric chloride followed by carbonization. Activated carbon FAC-1, FAC-2 and FAC-3 are prepared from sugarcane bagasse pith using different impregnation ratios (*SBP*: $FeCl_3$). It is found that adsorption of dye is influenced by several parameters such as initial dye concentration, contact time, solution *p*H, adsorbent dosage and adsorption temperature. Equilibrium adsorption isotherms and physico-chemical properties of the modified pith are investigated. Experimental adsorption data is correlated with Langmuir, Freundlich and Temkin isotherm models. Results of equilibrium experiments indicate that adsorption of methylene blue onto FAC-1, FAC-2 and FAC-3 is better described by Langmuir model and the maximum monolayer adsorption capacity at was 17 , 43 and 131 mg/g respectively. The thermodynamic parameters such as change in Gibbs free energy, enthalpy and entropy have also been evaluated and it has been found that the adsorption process was a spontaneous and exothermic in nature.

Keywords: Adsorption, Adsorption isotherm, Chemical activation, Methylene blue dye, Sugarcane bagasse pith, Thermodynamic

Synthetic dyestuffs are extensively used in textile, paper, pulp, printing, plastics, leather, cosmetics, pharmaceutical, food industries and dye houses[1]. These industries consume substantial volumes of water in order to colour their products, generating a considerable amount of colored wastewater[2]. More than 7,000 tons of approximately 10,000 different types of dyes and colored pigments are produced annually worldwide. Approximately 10-15% dyes are released into the environment during the dyeing process, making the effluent highly colored and aesthetically unpleasant. The effluent from a textile industry, thus carries a large number of dyes and other additives which are employed during the coloring process. Some of these dyes are carcinogenic and highly toxic to living organisms and posses certain hazard and environmental problems[3,4]. Hence colour removal from the industrial effluents has been the target of great attention in the last few years.

Several physico-chemical treatments have been applied for the removal of dyes from aqueous solutions such as ion-exchange, ultrafiltration, electrocoagulation, photooxidation, reverse-osmosis, microwave oxidation, etc. These procedures are associated with significant disadvantages, such as incomplete removal, high energy requirements and production of toxic sludge or waste products that also require disposal[5]. Among the physico-chemical processes, adsorption technology is considered to be one of the most effective and proven technology having potential applications in both water and wastewater treatment[6]. The use of commercial activated carbon is not suitable for wastewater treatment because of its high cost. Therefore, there is a need to produce activated carbon (AC) from cheaper and readily available materials.

Activated carbons are carbonaceous materials with highly developed internal surface area and porosity, sometimes described as solid sponges. The large surface area results in a high capacity for adsorbing chemicals from gases or liquids[7]. These properties are obtained when char is subjected to controlled gasification by oxidizing gases, or when a raw material impregnated with dehydrating agents is subject to carbonization.

India is an agricultural country generates a considerable amount of agricultural waste. Sugarcane bagasse - a fibrous waste left after juice extraction, available in large quantities and can be used as a raw material for the development of adsorbent. It is

divided into two major components - pith and rind. Pith is the inner part of sugarcane bagasse while the rind is the outer part[8]. Very few studies are available on the use of sugarcane bagasse pith based adsorbent for the removal of dye from wastewater[9,10]. Use of sugarcane bagasse based adsorbent would serve a double purpose. First, it converts surplus agricultural waste to useful a value-added product. Second, the produced activated carbon has wide applications in waste water treatment and other fields. This would contribute to solving some of the current day environmental pollution problems.

Two methods are widely used for the preparation of activated carbon: physical and chemical activation. Physical activation involves the carbonization of a precursor using gaseous activating agents such as steam or carbon dioxide. In chemical activation, the starting material is impregnated with an activating agent such as zinc chloride, sodium carbonate, potassium carbonate, alkali hydroxides, phosphoric acid, sulfuric acid and ammonium chloride etc. Impregnated material is heated in an inert atmosphere (nitrogen, carbon dioxide and argon)[11-13]. The chemical activation method is widely employed in preparation of activated carbon, mainly using the reagent zinc chloride as an activating agent. In this work the iron (III) salt, ferric chloride, was employed as an activating agent to produce activated carbon from sugarcane bagasse pith. Ferric chloride is the preferred over zinc chloride because of the environmental disadvantages associated with zinc chloride. Problems of corrosion and insufficient chemical recovery are also additional reasons. Zinc cation present in aqueous solution is a well-known pollutant. Ferric chloride has none of these disadvantages associated with it. Zinc is also higher in cost[14,15].

The objective of this work is to prepare low cost adsorbent from sugarcane bagasse pith by chemical activation method and to study its efficiency for dye removal. Simultaneously, it also solves the problems of disposal and pollution created by burning sugarcane bagasse waste. The adsorbent prepared was characterized by Fourier Transform Infrared (FTIR) spectroscopy, Scanning Electron Microscopy (SEM) with Energy Dispersive X-ray (EDX) analysis and Brunauer-Emmett-Teller (BET) method. Adsorption isotherm models such as Langmuir, Freundlich and Temkin were used to correlate the adsorption data. Thermodynamic studies were conducted to evaluate the methylene blue dye adsorption capacity of SBP based adsorbents.

Experimental Section

Materials

Sugarcane bagasse pith (SBP), used for the preparation of the activated carbon, was obtained from the Sahyadri Sahkari Sakhar Karkhana, Karad, India. The precursor was washed several times with distilled water to remove dirt from its surface, dried in an oven at 110°C until completely dry and then stored in sealed containers for experimentation.

Methylene Blue (MB) is a heterocyclic aromatic chemical compound with the molecular formula $C_{16}H_{18}N_3SCl{\cdot}3H_2O$($\lambda_{max}$: 665nm). Methylene blue (AR grade) supplied in powder form by S.D. Fine Chemical Ltd. (Boisor) was used without further purification. The structure of methylene blue dye is shown in Fig. 1. A UV-Visible spectrophotometer (Agilent Technologies, Model 8453, India) was used for determination of dye concentrations before and after adsorption. A *p*H meter (Equip-tronics digital *p*H meter, Model EQ-610) was used for pH measurements. The surface morphology of the adsorbent was observed using a JEOL JSM-6380LA analytical scanning electron microscope (SEM) technique. Brunauer-Emmett-Teller (BET) surface area, pore volume and pore size distribution were determined using the N_2 gas adsorption method with a Micromeritics ASAP 2020 Surface area and Porosity analyzer.

Determination of methylene blue dye concentration

A stock solution of 100 mg/L of methylene blue was prepared for calibration purposes. From the stock, different concentrations of methylene blue were prepared by diluting with distilled water. The concentrations of diluted solutions were analyzed spectrophotometrically by measuring their absorbance at the wavelength corresponding to maximum absorbance, λ_{max} = 665 nm. A calibration curve of absorbance against methylene blue concentrations was obtained by using standard methylene blue solutions of known concentrations at natural solution *p*H. The experimental data were fitted by a straight line with a high regression coefficient (R^2 = 0.998

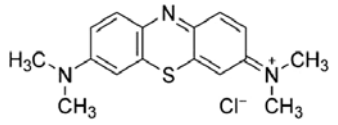

Fig. 1 — Chemical structure of methylene blue

and slope = 0.239). Replication measurements performed over a long time on fresh solutions prepared from the same initial mother solution resulted in perfectly coincident data.

Preparation of adsorbent

The washed and dried raw SBP material was soaked in ferric chloride solutions of different impregnation ratio (precursor material weight: ferric chloride weight) such as 1 : 0.2, 1 : 0.4 and 1 : 1 for 24 hr and then dried at 110°C for 6 hr to prepare impregnated material. The dried mixture was put into a cylindrical stainless steel reactor placed in a furnace and heated to 800°C under high purity N_2 flow (160 cm^3/min). The temperature was ramped at 10°C/min upto 800°C. This activation process was carried out for 1 hr. The activated product was then cooled to room temperature under N_2 flow. After cooling, the sample was treated with 0.1 M hydrochloric acid solution for 4 hr and then washed with distilled water until the *p*H of the washing solution reached until 6-7. Finally, the product was dried at 110°C for 8 hr, ground and sieved to a particle size of 60 meshes for further studies. The activated carbon prepared using 1:0.2, 1:0.4 and 1:1 impregnation ratios were named as FAC-1, FAC-2 and FAC-3 respectively. The percent yield was calculated using following Eqn. 1:

$$\% \, yield = \frac{m}{M} \times 100 \quad \ldots (1)$$

where m and M are the dry weights (g) of the activated carbon and the precursor, respectively (Table 1).

Adsorbent characterization

The infrared spectra of the sugarcane bagasse pith based activated carbon samples were obtained using a Fourier-transform infrared spectrometer (FT-IR, Perkin Elmer, USA). The samples were prepared as potassium bromide pellets and scanned over the range of 400-4000 cm^{-1} to identify the functional groups present on the surface of the carbon. The *p*H and conductivity were determined according to the standard method of ASTM D 3838-80 using electronic *p*H / conductivity meter (Labtronics, Model LT-23). The moisture content was determined according to ASTM 2867-99 method. Determination of iodine number was done according to the ASTM D 4607-94 method[16]. The point of zero charge (pH_{zpc}) of the adsorbent was determined by using *p*H drift method (Table 1).

Table 1 — Physico-chemical characteristics of adsorbents derived from SBP

Parameters	FAC-1	FAC-2	FAC-3
% Yield	33.5	36.5	38
Moisture content (%)	12.5	13.4	14
*p*H3	7-3.85	3.3-3.43	3.3-3.4
pH_{zpc}	5.02	3.97	3.66
Conductivity (**mS**)	0.074	0.147	0.227
Iodine number (**mg/g**)	152.6	185	601

Adsorption Studies

The batch adsorption experiments were conducted in temperature controlled constant shaking incubator (Neolab orbit shaker incubator) at shaking speed of 150 rpm using Erlenmeyer flasks at different concentrations of methylene blue solution and activated carbon loading. The effect of experimental conditions such as *p*H, temperature, contact time, adsorbent dose and initial dye concentrations on dye adsorption using FAC-1, FAC-2 and FAC-3 was studied. A stock solution of 1000 mg/L dye was prepared with distilled water and solutions of the required concentrations were prepared by successive dilution of the stock solution with distilled water. The adsorption experiments were conducted at room temperature (30°C) and *p*H of the solutions was 5.7 ± 0.3. The effect of initial *p*H on dye removal was studied over the *p*H range of 3 - 9. The initial *p*H of the dye solution was adjusted by the addition of 0.1 M hydrochloric acid or 0.1 M sodium hydroxide. In order to determine the effect of temperature on adsorption process, 10 g/L (FAC-1 and FAC-2, C_0=50 mg/L) and 5 g/L (FAC-3**,** C_0=650 *mg/L*) carbon was dosed by varying temperature from 30°C to 50°C. The effect of contact time and initial dye concentration on adsorption was determined at different time intervals over the time range of 15 – 240 min. The effect of adsorbent dosage on dye adsorption was studied by varying the amount of adsorbent from 0.25 to 1.00 g. The equilibrium isotherm studies were performed by loading 10 g/L (FAC-1 and FAC-2) and 5 g/L (FAC-3) of activated carbon into solution of different initial concentrations of methylene blue at *p*H 5.7 ± 0.3. The flasks were shaken for 24 hr to attain equilibrium. The thermodynamic experiments were carried out at three different temperatures, i.e., 30, 40 and 50°C using 5 g/L of carbon dosage for dye of known concentration. All the experiments were duplicated and showed differences of less than 4.0% (Table 1).

The amount of dye adsorption at equilibrium (Q_e, mg/L), Eq. 2 and at any time, t, (Q_t, mg/L), Eq. 3, and dye removal percentage, Eq. 4 was calculated by following equations[17]:

$$Adsorption\ Uptake,\ Q_e = \frac{(C_0 - C_e)V}{m} \quad \ldots (2)$$

$$Adsorption\ Uptake,\ Q_t = \frac{(C_0 - C_t)V}{m} \quad \ldots (3)$$

$$Dye\ removal\ \% = \frac{(C_0 - C_t)}{C_0} \times 100 \quad \ldots (4)$$

where C_0, C_t and C_e (mg/L) and are the initial, at any time t and equilibrium concentrations of methylene blue, respectively. V (L) is the volume of the dye solution and m (g) is the mass of adsorbent added.

Desorption experiments

Desorption of the adsorbed methylene blue dye was carried out using a solvent desorption method. In the solvent desorption study, the dye loaded FAC-3 was separated from the solution and washed with distilled water. The carbon sample was dried completely and used for desorption experiments. The dye loaded FAC-3 (0.1 g) was agitated at 150 rpm in 100 mL conical flasks containing 25 mL of 0.1 N HCl, 0.1 N NaOH, 0.1 N H_2SO_4, distilled water, methanol and acetone at 30°C for 24 hr in the orbital shaker.

Results and Discussion

Effect of chemical impregnation ratio

The effect of the chemical impregnation ratio on the pore structure and surface area of the prepared activated carbons was investigated by using the standard Brunauer– Emmett–Teller (BET) method. Values of surface area and pore characteristics of all three carbon materials are tabulated in Table 2 The external surface area, pore width, pore diameter shows a slight increase as the SBP : ferric chloride ratio was raised from 1 : 0.2 to 1 : 1. The total surface area of the activated carbon samples was less affected by impregnation ratio. This might be due to the coalescence of micropores into mesopores, resulting in slightly increase in surface area[18]. The Barett-Joyner-Halenda (BJH) method is one of the most commonly used means to describe the mesopore size distribution[19]. However, the total pore volume as well as the mesopore volume was increased from 0.05 to 0.168 (cm^3/g) with an increasing activating agent. The pores in the carbon matrix can be created by removing the chemical activating agent from the carbonized sample. Also, the iodine adsorption capacity was increased from 152.6 to 601 mg/g with impregnation ratio. Thus, the results suggested that an excess of ferric chloride could induce the pore widening, leading to the formation of a mesoporous structure, resulting in increased iodine as well as methylene blue dye adsorption.

Activated carbon characterization

FTIR spectra

The FTIR spectra of raw bagasse pith, FAC-1, FAC-2 is shown in Fig. 2, similar results were

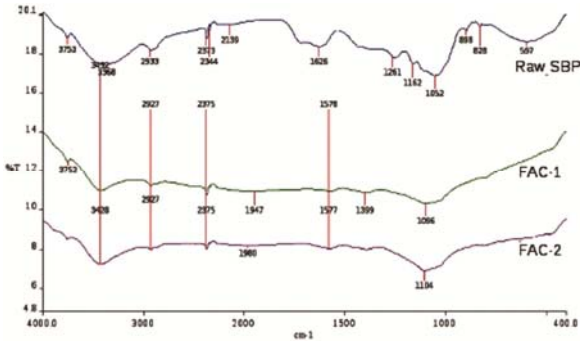

Fig. 2 — FTIR spectra of SBP and SBP based activated carbon

Table 2 — Surface area and pore characteristics of SBP based adsorbents

BET parameters	FAC-1	FAC-2	FAC-3
BET surface area (m^2/g)	346.16	341.75	519.23
Single point surface area at P/P_0 (m^2/g)	355.88	349.76	527.56
Langmuir surface area (m^2/g)	483.84	479.47	731.5
t-Plot micropore surface area (m^2/g)	307.9	274.3	391
t-Plot external surface area (m^2/g)	38.3	67.5	128.3
Total pore volume (cm^3/g)	0.203	0.25	0.36
t-Plot micropore volume (cm^3/g)	0.152	0.135	0.19
t-Plot mesopore volume (cm^3/g)	0.05	0.112	0.168
BJH adsorption average pore diameter, $4V/A$ by BET (nm)	8.86	10.0.4	8.0
BJH desorption average pore diameter, $4V/A$ by BET (nm)	9.93	10.5	7.7
Pore width $4V/A$ by BET (nm)	2.35	2.9	2.77

obtained with FAC-3. The broad and intense peak at 3752 - 3432 cm^{-1} is assigned to intra and inter molecular hydrogen bonded (*−OH*) stretching of hydroxyl group that occur in cellulose[20]. The peak observed at 2927 cm^{-1} indicates the presence of C-H asymmetric stretching of CH_3 and CH_2 groups[21]. The peaks at 2375 cm^{-1} indicates the presence of *−C≡C−H* alkyne stretching; the band 2344 cm^{-1} is attributed to *C=O* asymmetric stretching vibration of CO_2, which was absent in activated carbon samples due to carbonization at high temperature. The bands located at 2139, 1980, 1947 cm^{-1} corresponds to *C=O* is stretching of carboxylic acid group. The peaks at 1626 and 1578 cm^{-1} suggest the *C=C* stretching of aromatic ring and *C=O* stretching of the carbonyl group. The peaks observed between 1399 to 1052 cm^{-1} indicates the presence of *C−O* stretching and *C−OH* bending vibrations of alcohols and carboxylic acids[22]. The band at 898-828 cm^{-1} could be *O−O* stretching, while the band at 596 cm^{-1} suggests the C-heteroatom vibrations. So, *C=O*, *−COO−* and *C−O* seem to participate in the methylene blue binding. Thus, the FT-IR spectrum of FAC-1, FAC-2 and FAC-3 confirms that carboxyl and hydroxyl groups are present in abundance. These groups are expected to play a key role in the adsorption of dye.

Surface morphology of activated carbon

SEM has been a primary tool for characterizing the surface morphology of the adsorbent surface. Figure 3 shows the SEM images of the raw sugarcane bagasse pith, FAC-1, FAC-2 and FAC-3. Large and well developed pores were clearly found on the surface of the activated carbon. This might be due to activation process used, which involved the chemical activating agent. Pore development in the char during pyrolysis was also important as this would enhance the surface area and pore volume of the activated carbon. This promoted the diffusion of ferric chloride molecules into the pores and thereby increasing the $FeCl_3$-carbon reaction, which would then create more pores in the activated carbon. From EDX analysis, it can be clearly seen that some of the iron metals found to be trapped at the surface of the activated carbon and also showed the presence of calcium, magnesium, chlorine elements. The well developed pores found in the prepared activated carbon could be the main factor that had lead to the high methylene blue dye uptake in this study.

Surface area analysis (BET)

The nitrogen adsorption/desorption isotherm of the obtained adsorbents is seen in fig. 4. The activated carbon samples were characterized by specific surface

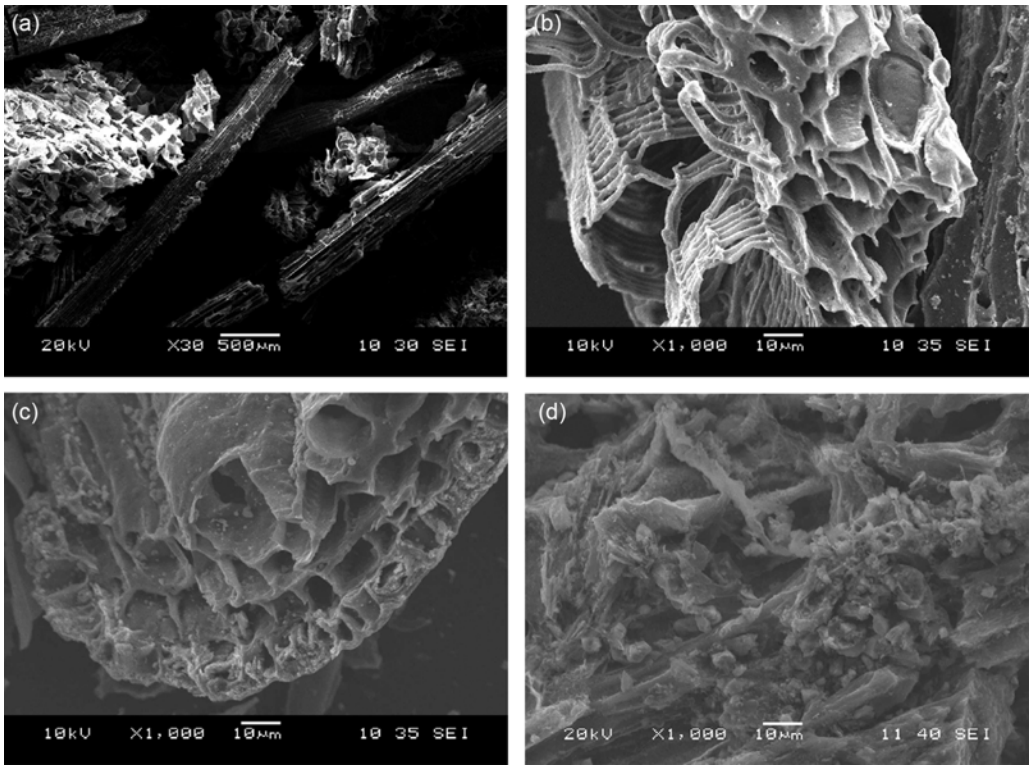

Fig. 3 — SEM images of (a) $SBP_{untrated}$, (b) FAC-1, (c) FAC-2 and (d) FAC-3

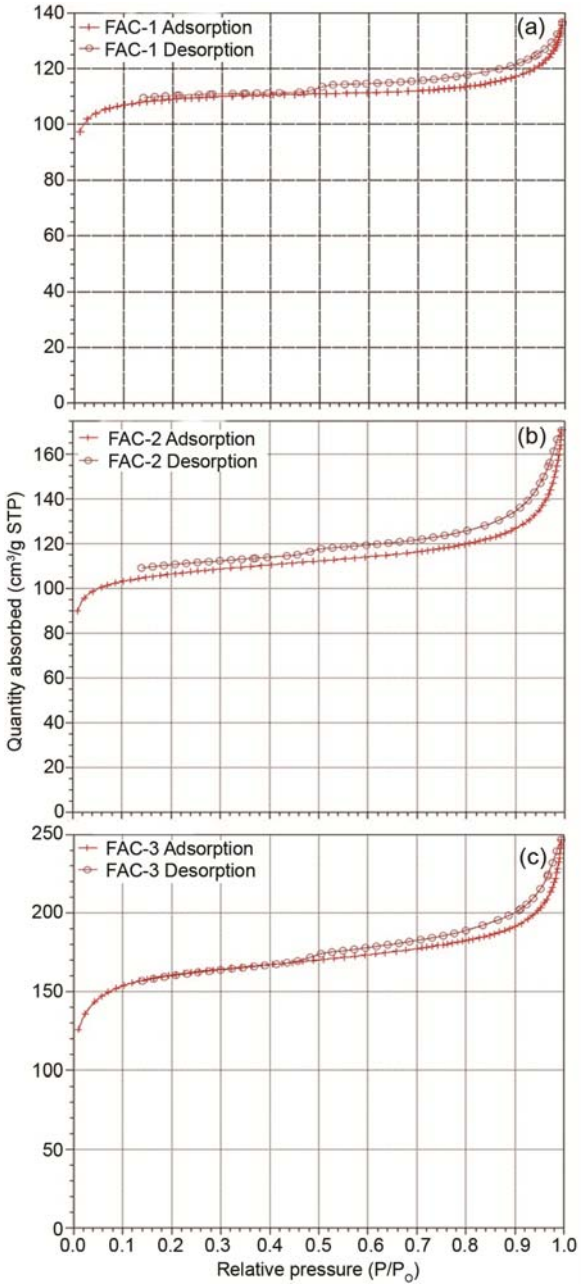

Fig. 4 — Nitrogen adsorption /desorption isotherm of (a) FAC-1, (b) FAC-2 and (c) FAC-3

area, pore volume and pore diameter. These values were measured at –195.45°C using N_2 adsorption–desorption isotherm. The specific surface area of FAC-1, FAC-2 and FAC-3 has been calculated by the standard Brunauer– Emmett–Teller (BET) method and it was found to be 346.2, 341.7 and 519.23 m^2/g respectively. The average pore diameter was determined using the equation $\frac{4V}{A}$, where A is the BET surface area and V is the single point total pore volume. The porosity is classified by IUPAC into three different groups of pore sizes. Micropores: a width less than 2 nm, mesopores: width between 2 - 50 nm and macropores: greater than 50 nm wide[23]. On the other hand, N_2 adsorption isotherm indicates that all three samples fall within type IV isotherm, typical of mesoporous solids. The volume of mesopores was calculated by subtracting the volume of microspores from the total pore volume at $\frac{P}{P_o} = 0.99$. The total pore volume gradually increases, suggesting that the pores are widened and the pore size distribution becomes broader[24]. Table 2 illustrates the surface area and pore characteristics, including BET surface area (S_{BET}), micropore surface area (S_{micro}), total pore volume (V_T), micropore volume (V_{micro}), mesopore volume (V_{meso}) and pore width ($\frac{4V}{A}$ by BET). Table 2 reveals that the obtained adsorbents have a mesoporous structure.

Zero point charge (pH_{ZPC})

The *p*H at the potential of zero charge of the prepared activated carbon (pH_{ZPC}) was determined using the *p*H drift method[25, 26]. To measure the pH_{ZPC} of the carbon samples, 40 mL of 0.1 M sodium chloride solution at *p*H 7 was taken. The *p*H of the solution of 0.1 M sodium chloride was adjusted between 3 and 11 by using 0.01 M sodium hydroxide and 0.1 M hydrochloric acid. N_2 was bubbled through the solution to remove the dissolved carbondioxide. 0.2 g sample was added to each flask and shaken for 24 hr to an orbital shaker at 25°C, the final *p*H was recorded. The graph of final *p*H verses initial *p*H was used to determine the point at which initial and final *p*H values were equal. This was taken as a zero point charge of the activated carbon pH_{ZPC} and values showed in Table 1. The activated carbon surface will be positively charged at $pH < pH_{ZPC}$ and negatively charged at $pH > pH_{ZPC}$. Table 1 emphasize that obtained adsorbents have positively charged surface.

Effect of operating conditions on adsorption

Effect of pH

The initial *p*H of the aqueous medium is an important factor that may affect the uptake of the adsorbate. The acidity of the solution, influenced the surface charge of the adsorbent, the degree of ionization of the material present in the solution and

surface chemistry of the adsorbent. Studies were carried out to see the effect of *p*H in the range 3 - 9. Figure 5 shows the effect of the initial *p*H of the dye solution on the adsorption capacity of adsorbents. It was observed that, the adsorption of methylene blue by all three adsorbents is higher at *p*H 7. At lower *p*H, the concentration of the hydrogen ions is higher and the adsorbent surface becomes positively charged thus, the repulsion of positively charges inhibits the adsorption of dye cation. At higher *p*H, the surface of adsorbent becomes more negatively charged, due to this, the presence of other cation in solution competes with dye cation causing a decrease in the amount of dye adsorbed. Similar trends were reported in the literature for the adsorption of methylene blue dye using Calotropis Gigantea based adsorbent[27].

Effect of contact time and initial dye concentration

Initial dye concentration is one of the important factors that affect the adsorption capacity. Figure 6a, 6b and 6c shows the effect of contact time and initial dye concentration on the adsorption capacity of methylene blue onto FAC-1, FAC-2 and FAC-3 respectively. Studies were carried out at different initial concentrations without changing the initial *p*H of the medium. It was found that, percent dye adsorption increased with contact time, but however, decreased with increase in initial dye concentration. Also, it was clear that, the extent of adsorption is rapid in the initial stages and becomes slow in later stages. During adsorption of dyes, initially the dye molecules reach the boundary layer; then they have to diffuse into the adsorbent surface; and finally they have to diffuse into the porous structure of the adsorbent. Hence this phenomenon will take a relatively longer contact time. Figure 6a, 6b and 6c reveals that the curves are single, smooth, and continuous, leading to saturation, suggesting the possible monolayer coverage of the methylene blue dye on the carbon surface[28].

Effect of adsorbent dose

The percentage removal of methylene blue dye was studied by varying the adsorbent dose between 0.25 and 1.00 g at an initial dye concentration of 100 mg/L and 1000 mg/L. The results depicted in Fig. 7 shows that removal efficiency was increased with increasing the amount of carbon. It was observed that, the dye removal percentage increases from 23.12 to 60.46% for FAC-1, 43.46 to 91.75% for FAC-2 and 28 to 93.8% for FAC-3 as the adsorbent amount increases from 0.25 to 1.00 g. This trend is expected because as

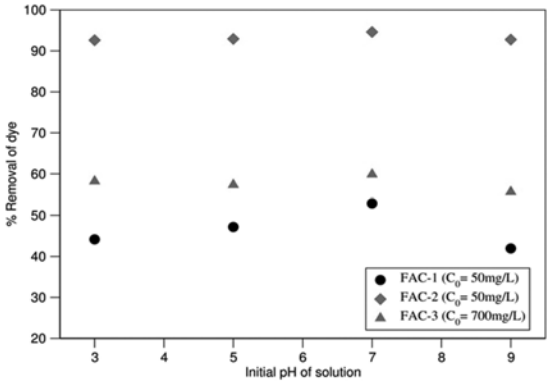

Fig. 5 — Effect of initial pH of solution on MB adsorption

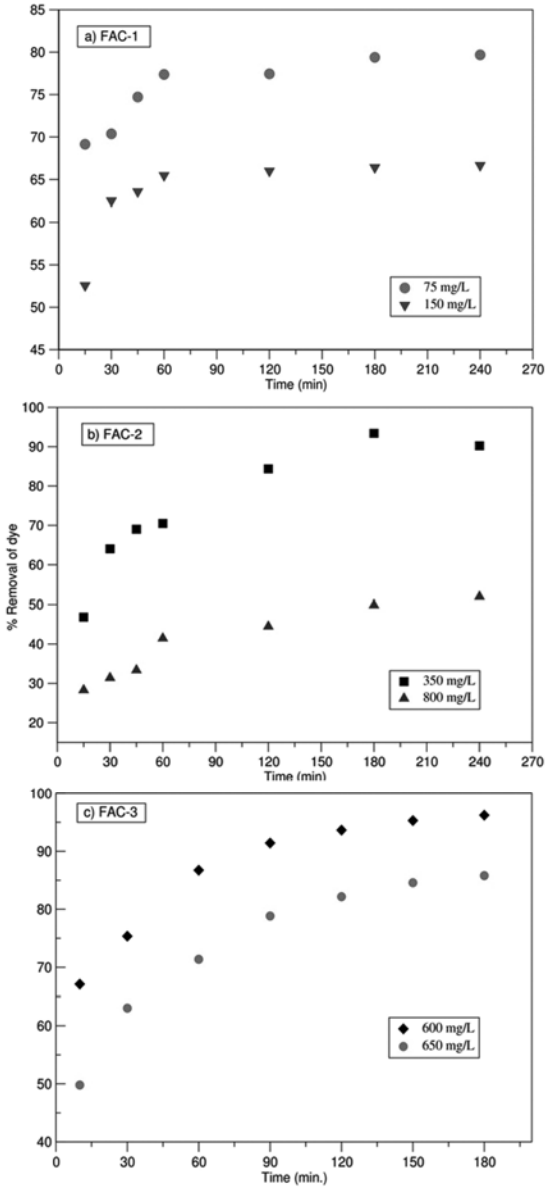

Fig. 6 — Effect of contact time and initial concentration on MB adsorption (a) FAC-1, (b) FAC-2 and (c) FAC-3

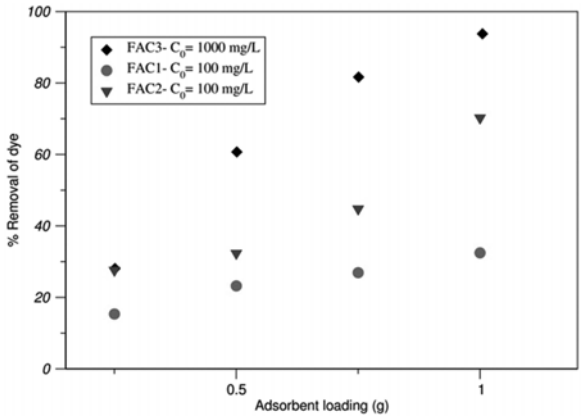

Fig. 7 — Effect of amount of activated carbon on MB adsorption

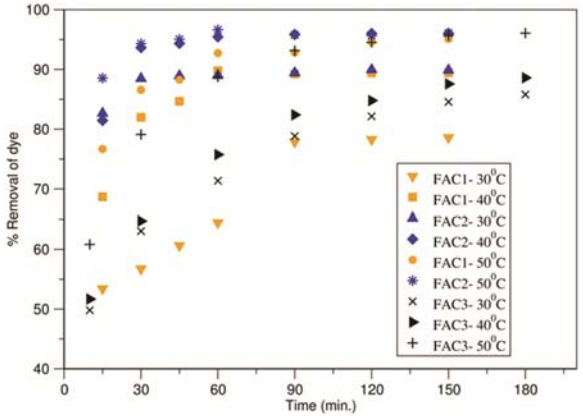

Fig. 8 — Effect of temperature on MB adsorption

the adsorbent dose increases the number of adsorption sites also increases and thus more dye gets adsorbed to the surface.

Effect of temperature

The temperature has important effects on adsorption process. The effect of temperature on dye adsorption onto all three activated carbon materials was investigated at three different solution temperatures (30 – 50°C). The dye adsorption capacities of all three adsorbents were increased with temperature. The result, as depicted in Fig. 8, clearly indicates that dye removal percentages increases with temperature. Also, we can see the removal efficiency, increased from 78.7 to 95, 89.9 to 96 and 85.5 to 96% with FAC-1, FAC-2 and FAC-3 samples respectively. Two reasons could explain these results. First, the increase in temperature enhances the rate of diffusion of the adsorbate molecules across the external boundary layer and in the internal pores of the adsorbent particles. Second, the mobility of adsorbate molecules also increases with temperature, thereby facilitating the formation of surface monolayers resulting in increased adsorption[29].

Adsorption isotherms

The equilibrium adsorption isotherms are one of the promising technique to understand the mechanism of the adsorption. The adsorption isotherm indicates how the adsorption molecules are distributed between the liquid phase and the solid phase when the adsorption process reaches an equilibrium state. The fitness of the equilibrium adsorption data obtained from the experiments at 30°C was correlated with the Langmuir, Freundlich and Temkin isotherm models. The applicability of the isotherm equations was compared by judging the correlation coefficient, R^2.

Langmuir isotherm

The Langmuir isotherm is valid for monolayer adsorption onto completely homogeneous surfaces without interaction between adsorbed molecules[30]. The model is based on several basic assumptions: (i) the adsorption takes place at specific homogenous sites within the adsorbent; (ii) once a dye molecule occupies a site; (iii) the adsorbent has a finite capacity for the adsorbate (at equilibrium); (iv) all sites are identical and energetically equivalent. Therefore, the Langmuir isotherm model was chosen for estimation of the maximum adsorption capacity corresponding to complete monolayer coverage on the adsorbent surface[31]. The expression of the Langmuir isotherm model is given by Eq. 5.

$$Q_e = \frac{Q_m K_a C_e}{1 + K_a C_e} \quad \ldots (5)$$

where Qe (mg/g) and C_e (mg/L) are the amount of adsorbed adsorbate per unit mass of adsorbent and unadsorbed adsorbate concentration in solution at equilibrium, respectively. Q_e (mg/g) is the maximum sorption capacity corresponding to complete monolayer coverage and K_a is the equilibrium constant related to the energy of adsorption (L/g). The plot of Q_e verses was shown in Fig. 9. The constants Q_m and K_a can be calculated from the slope and intercept of the plot and the values are tabulated in Table 3.

The essential characteristics of the Langmuir isotherm can be expressed in terms of a dimensionless equilibrium parameter (R_L)[32], which is defined in Eq. 6 as:

$$R_L = \frac{1}{1 + K_a C_0} \quad \ldots (6)$$

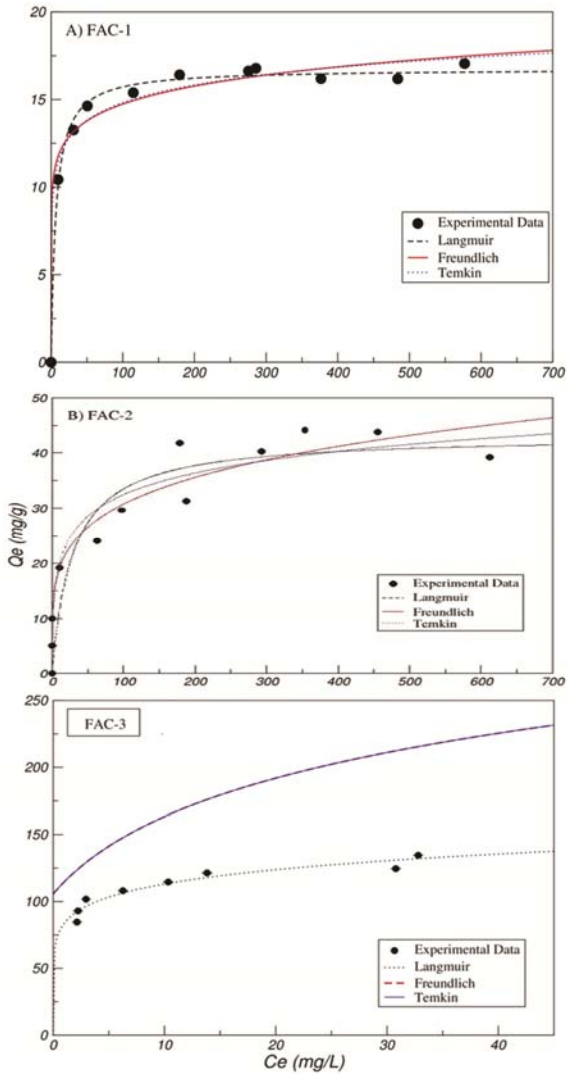

Fig. 9 — Equilibrium adsorption isotherm of MB onto (a) FAC-1, (b) FAC-2 and (c) FAC-3 at 30˚C

Table 3 — Results of isotherm parameters of MB adsorption at 30℃

Isotherm models	Isotherm constants	FAC-1	FAC-2	FAC-3
Langmuir	Q_m (mg/g)	17	43	131
	K_a (L/g)	0.153	0.034	0.97
	R_L	0.009-0.054	0.028-0.362	0.001-0.002
	R^2	0.997	0.96	0.961
Freundlich	k_f (mg/g)	9.43	11.62	83.74
	$1/n$	0.097	0.22	0.13
	R^2	0.99	0.96	0.96
Temkin	A_T (L/g)	253.6	3.095	12.67
	B (L/g)	1.46	5.66	35.17
	b_T (J/mol)	1723	445	71.63
	R^2	0.95	0.958	0.93

where K_a is the Langmuir constant and C_0 is the highest dye concentration (mg/L). The value of R_L indicates the type of the isotherm to be either unfavorable (R_L > 1), Linear (R_L=1) favorable (0 < R_L < 1) or irreversible (R_L=0)[33]. In the present investigation, R_L values were less than 1 which confirmed that the adsorbents prepared from the sugarcane bagasse pith is favorable for adsorption.

Freundlich isotherm

The Freundlich equilibrium isotherm was also used to describe the experimental adsorption data. This isotherm model assumes a heterogeneous surface with a non-uniform distribution of heat of adsorption over the surface[34]. The Freundlich Eq. 7 can be represented as follows:

$$Q_e = k_f C_e^{1/n} \quad \ldots \quad (7)$$

where Q_e(mg/g) and C_e(mg/L) are defined as the amount of dye adsorbed per unit weight of adsorbent and equilibrium liquid-phase concentration, respectively. k_f(mg/g) ,is an indication of the multilayer adsorption capacity and $\frac{1}{n}$ is an adsorption intensity. The Freundlich exponent, n, should have values lying in the range of 1 to 10 for classification as favorable adsorption. The value of $\frac{1}{n}$ ranging between 0 and 1 is a measure of adsorption intensity or surface heterogeneity and becomes more heterogeneous as its value gets closer to zero[35]. The values of k_f and n can be calculated from the slope and intercept respectively. The non-linear form of this model is shown in Fig. 9 and its parameters are also shown in Table 3. From intercept, the adsorption intensity ($\frac{1}{n}$) of FAC-1, FAC-2 and FAC-3 was found to be 0.097, 0.2112 and 0.13 respectively, which revealed the favorable adsorption.

Temkin isotherm

This isotherm contains a factor that explicitly taking into the account of adsorbent–adsorbate interactions. As implied in the equation, its derivation is characterized by a uniform distribution of binding energies. Fitting was carried out by plotting the quantity adsorbed Q_e against lnC_e and the constants were determined from the slope and intercept[36]. The model is given by the following Eq. 8:

$$Q_e = \frac{RT}{b_T} \ln(A_T C_e) \quad \ldots (8)$$

where A_T is the Temkin isotherm equilibrium binding constant (L/g), b_T is the Temkin isotherm constant, R is the universal gas constant (8.314 J/molK), $T°K$ is the absolute temperature, B is the constant related to heat of sorption (*J/mol*). These parameters were calculated by non-linear regression fitting as shown in Fig. 9, A_T and b_T are recorded in Table 3.

Adsorption thermodynamics

The adsorption capacity of the carbon increased with an increase in the temperature of the system from 30–50°C. The thermodynamic parameters such as change in Gibbs free energy (ΔG°), enthalpy change (ΔH°) and entropy change (ΔS°) were calulated using following equations[37, 38].

$$\Delta G° = -RT \ln K_c \quad \ldots (9)$$

Van't Hoff equation:

$$\ln K_c = \frac{\Delta S°}{R} - \frac{\Delta H°}{RT} \quad \ldots 10)$$

Gibbs–Helmholtz equation:

$$\Delta G° = \Delta H° - T\Delta S° \quad \ldots (11)$$

where K_c is the equilibrium constant of the adsorption, is equal to $(\frac{Q_e}{C_e})$. R is the gas constant (8.314 *J/molK*)and T is the temperature in Kelvin. The plot of K_c vs $\frac{1}{T}$ is linear with the slope and y-intercept giving values of $\Delta H°$ and ΔS° (Fig. 10). The magnitude of $\Delta G°$ was calculated from Gibbs-Helmholtz equation. The calculated values of $\Delta G°$, $\Delta H°$ and $\Delta S°$ and are listed in Table 4.

The negative values of change in Gibbs free energy ($\Delta G°$) and enthalpy change ($\Delta H°$) indicate that the adsorption of dye was a spontaneous and exothermic. It was expected that adsorption processes (either from gas or liquid phase) are exothermic due to the heat released after bond formation between solute and adsorbent[39]. The positive value of entropy change ($\Delta S°$) suggests increased randomness at the solid/solution interface during adsorption[40].

Desorption study

Various solvents, namely, HCl, NaOH, H_2SO_4 distilled water, methanol and acetone were used in the elution of methylene blue dye from FAC-3. However, acetone and methanol showed some desorption efficiency and the per cent desorption for dye was found to be 0.31 and 19.26 respectively.

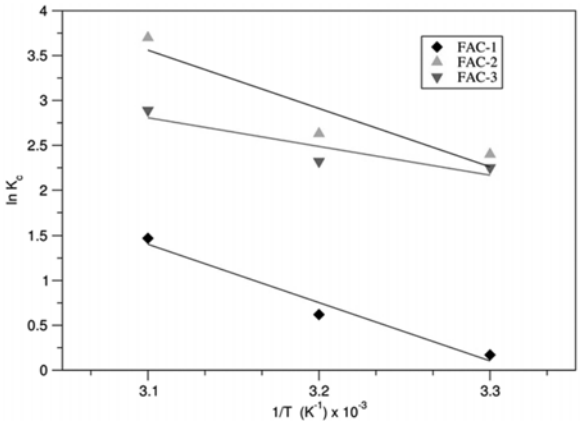

Fig. 10 — Van't Hoff plots for adsorption MB on SBP adsorbents

Table 4 — Thermodynamic parameters for the adsorption of MB onto SBP adsorbents

Adsorbents	Temp. (°K)	K_c (L/g)	ΔG^0 (kJ/mol)	ΔH (kJ/mol)	ΔS^0 (kJ /mol. K)
FAC-1	303	1.19	- 0.43	- 0.088	0.301
	313	1.86	- 1.62		
	323	4.33	- 3.93		
FAC-2	303	10.98	- 6.04	- 1.23	4.115
	313	13.92	- 6.85		
	323	40.55	- 9.94		
FAC-3	303	9.48	- 5.67	- 0.027	0.105
	313	10.2	- 6.04		
	323	18.07	- 7.78		

Table 5 — Comparison of adsorption capacities of different adsorbents for MB

Adsorbents	Adsorption capacities (mg/g)	References
Lantana camera stem	19.84	41
Delonix regia pods	23.3	42
Palm Kernel shell	3.22	3
Bamboo charcoal	17.32	43
Ashoka leaf powder	90.9	5
Cola nut shells	87.12	44
Sugarcane bagasse pith		Present work
FAC-1	17	
FAC-2	43	
FAC-3	131	

Comparison with the other adsorbents reported in literature

The adsorption capacities of various low cost adsorbents for methylene blue dye adsorption as reported in the literature are presented in Table 5. A

comparison between this work and the reported data from the literature shows that FAC-3 shows better methylene blue dye adsorption capacity than other adsorbents. Therefore, it could be safely concluded that the sugarcane bagasse pith based activated carbon has a considerable potential for removal of dyes from water and wastewater.

Conclusion

The results of this investigation show that activated carbon derived from agro-industrial waste, sugarcane bagasse pith was successfully utilized for methylene blue adsorption. The adsorption of methylene blue dye onto FAC-1, FAC-2 and FAC-3 has been studied. Batch adsorption experiments demonstrated that the adsorption is affected by various parameters such as contact time, solution *p*H, temperature, adsorbent dosage and initial dye concentration. The following conclusions are drawn based on the results of the present study:

1. Sugarcane bagasse pith like other agricultural, industrial waste has been successfully used for low cost bioadsorbent preparation and can be used in the treatment process of dye in waste water.
2. Maximum methylene blue dye removal percentage (80%) is attained at initial 120 minutes and optimum adsorption capacity at *p*H 7.
3. The adsorption isotherms suggest that Langmuir isotherm better explained the experimental data of methylene blue than Freundlich and Temkin isotherms. The value of the maximum adsorption capacity Q_m calculated from the Langmuir model is also closer to the experimental value of Q_m than that of other models and confirmed that adsorption is monolayer.
4. Textural morphology of activated carbon determined by the SEM-EDX clearly showed that the activated carbon was full of cavities. Some iron metals are found at the surface of the activated carbon.
5. Thermodynamic studies indicated that the methylene blue dye adsorption onto SBP adsorbents is a spontaneous and exothermic.
6. The SBP adsorbents are hereby presented as a mesoporous adsorbent with high pore volume and specific surface area from a low cost agricultural biomass.

Therefore, it can be concluded that adsorbents derived from sugarcane bagasse pith show promising applications in the control of water pollution and represent as an economical and environment friendly technique. Hence scalable for industrial purpose.

Acknowledgement

The authors would like to gratefully acknowledge the Department of Science and Technology (DST), Government of India for their financial support under DST-FIST program (SR/FST/ETII/007-2007). One of the authors (MBA) is grateful to University Grants Commission (UGC), Government of India, New Delhi, for research fellowship (F.4-1/2006(BSR)/8-10/2007/BSR).

List of symbols

C_e - Unadsorbed dye concentration in solution at equilibrium, mg/L

C_0 - Initial dye concentration, mg/L

C_t - Dye concentration in solution at time t, mg/L

Q_e - Equilibrium solid-phase concentration, mg/L

Q_m - Maximum monolayer adsorption capacity, mg/g

K_a - Langmuir equilibrium constant, L/g

kf - Freundlich isotherm constant, mg/g

$\frac{1}{n}$ - Adsorption intensity

Q_t - Solid-phase concentration at any time t, mg/g

A_T - Temkin isotherm equilibrium binding constant, L/g

b_T - Temkin isotherm constant, J/mol

V - Liquid-phase volume, L

m - Mass of the adsorbent, g

M - Mass of the sugarcane bagasse pith, g

t - Time in min

R_L -Separation factor

R^2 - Regression coefficient

T - Absolute temperature, K

R -Universal gas constant, J/molK

K_c - Equilibrium constant of the adsorption, L/g

$\Delta G°$ - Change in Gibbs free energy of the adsorption reaction, kJ/mol

$\Delta H°$ - Enthalpy change of the adsorption reaction, kJ/mol

$\Delta S°$- Entropy change of the adsorption reaction, kJ/molK

Reference

1 Gao J, Qin Y, Zhou T, Cao D, Xu P, Hochstetter D & Wang Y, *J Zhejiang Univ Sci B*, 14 (2013) 650.

2 Chowdhury S & Das P, *Environ. Prog. Sustain. Energy*, 31 (2012) 415.

3 Abechi S E, Gimba C E, Uzairu A, Kagbu J A & Ocholi O J, *Int Refereed J Eng Sci*, 2 (2013) 38.

4 Ratna & Padhi B S, *Int J Environ Sci*, 3 (2012) 940.

5 Gupta N, Kushwaha A K & Chattopadhyaya M C, *J Taiwan Inst Chem Eng*, 43 (2012) 604.

6 Samarghandi M R, Hadi M, Moayedi S & Askari F B, *Iran J Environ Health Sci Eng*, 6 (2009) 285.

7 Zanzi R, Bai X, Capdevila P & Bjornbom E, *6th World Congress of Chem Eng Melbourne, Australia*, (2001) 23.

8 Krishnan K A & Anirudhan T S, *Water SA*, 29 (2003) 147.
9 Ho Y S & Mckay G, *Resour Conserv Recy*, 25, (1999) 171.
10 Amin N K, *Desalination*, 223 (2008) 152.
11 Moussavi G, Alahabadi, Yaghmaeian K & Eskandari M, *Chem Eng J*, 217 (2013) 119.
12 Venkata Ramana D K, Reddy D H, Yu J S & Seshaiah K, *Chem Eng J*, 197 2012) 24.
13 Guo J & Lua A C, IChemE, 81 (2003) 585.
14 Oliveira L C, Pereira E, Guimaraes I R, Vallone A, Pereira M, Mesquita J P & Sapag K, *J Hazard Mater*, 165 (2009) 87.
15 Yakout S M & Sharaf El-Deen G, *Arabian J Chem*, (2012) 1.
16 Verla A W, Horsfall M, Verla M E, Spiff A & Ekpete O, *Asian J Natural Appl Sci*, 1 (2012) 39.
17 Fu J, Chen Z, Wang M, Liu S, Zhang J, Han R & Xu Q, *Chem Eng J*, 259 (2015) 53.
18 Buasri A, Chaiyut N, Loryuenyong V, Phakdeepataraphan E, Watpathomsub S & Kunakkemakorn V, *Int J Chem Nucl Mater Metall Eng*, **7** (2013) 98.
19 Qian Q, Machida M, Aikawa M & Tatsumoto H, *J Mater Cycles waste Manag*, 10 (2008) 53.
20 Malik R, Ramteke D S & Wate S R, *Indian J Chem Technol*, 13 (2006) 319.
21 Sidik S M, Jalil A A, Triwahyono S, Adam S H, Satar M A & Hameed B H, *Chem Eng J*, 203 (2012) 9.
22 Yao Z Y, Qi J & Wang L H, *J Hazard Mater*, 174 (2010) 137.
23 Liou T H & Wu S J, *J Hazard Mater*, 171 (2009) 693.
24 Zhonghua H & Srinivasan M P, *Microporous Mesoporous Mater*, 43 (2001) 267.
25 Baskaran P K, Venkatraman B R & Arivoli S, *E J CHEM*, 8 (2011) 9.
26 Karthikeyan G & Ilango S S, *Iran J Environ Health Sci Eng*, 4 (2007) 21.
27 Abedi M & Bahreini Z, *World Appl Sci J*, 11 (2010) 263.
28 Arivoli S, Hema M, Parthasarathy S & Manju N, *J Chem Pharm Res*, 25 (2010) 626.
29 Patil S, Deshmukh V, Renukdas S & Patel N, *Int J Environ Sci*, 1 (2011) 1116.
30 Li Q, Chai L & Qin W, *Chem Eng J*, 197 (2012) 173.
31 Khaled A, El-Nemr A, El-Sikaily A & Abdelwahab O, *J Hazard Mater*, 165 (2009) 100.
32 Hameed B H, Din A T M & Ahmad A L, *J Hazard Mater*, 141 (2007) 819.
33 Mylsamy S & Thievarasu C, *World J Appl Environ Chem*, 1 (2012) 22.
34 Suyamboo B & Perumal R, *Iran J Energy Environ*, 3 (2012) 23.
35 Achmad A, Kassim J, Suan T K, Amat R & Seey T L, *J Phys Sci*, 23 (2012) 1.
36 Dada A O, Olalekan A P, Olatunya A M & Dada O, *J Appl Chem*, 3 (2012) 38.
37 Al-Degs Y S, El-Barghouthi M I, El-Sheikh A H & Walker G A, *DYES PIGMENTS*, **77** (2008) 16.
38 Sulak M T & Yatmaz H C, *DESALIN WATER TREAT*, 37 (2012) 169.
39 Ruthven D M, *Principles of adsorption and adsorption processes*, JOHN WILEY and SONS, 1984.
40 N. M. Mahmoodi, B. Hayati, M. Arami & C. Lan, *Desalination*, 268 (2011) 117.
41 O. S. Amuda, A. O. Olayiwola, A. O. Alade, A. G. Farombi & S. A. Adebisi, *J Environ Prot*, 5 (2015) 1352.
42 Ho Y, Malarvizhi R & Sulochana N, *J Environ Prot Sci*, 3 (2009) 111.
43 Liao P, Ismael Z M, Zhang W, Yuan S, Tong M, Wang K & Bao J, *Chem Eng J*, 195-196 (2012) 339.
44 Nsami J N & M badcam J K, *J Chem*, 2013 (2013) 1.